BIOCHEMISTRY
including biophysical chemistry & molecular biology

Article

pubs.acs.org/biochemistry

Agonist and Antagonist Binding in Human Glycine Receptors

Rilei Yu,[†] Eliott Hurdiss,[‡] Timo Greiner,[‡] Remigijus Lape,[‡] Lucia Sivilotti,*[,‡] and Philip C. Biggin*[,†]

[†]Structural Bioinformatics and Computational Biochemistry, Department of Biochemistry, University of Oxford, South Parks Road, Oxford OX1 3QU, United Kingdom

[‡]Neuroscience, Physiology and Pharmacology, University College London, Medical Sciences Building, Gower Street, London WC1E 6BT, United Kingdom

Supporting Information

ABSTRACT: The human glycine receptor (hGlyR) is an anion-permeable ligand-gated channel that is part of a larger superfamily of receptors called the Cys-loop family. hGlyRs are particularly amenable to single-channel recordings, thus making them a model experimental system for understanding the Cys-loop receptor family in general. Understanding the relationship between agonist binding and efficacy in Cys-loop receptors should improve our future prospects for making specific agonists or antagonists. However, at present, there is no high-resolution structure for the complete hGlyR, and thus, modeling is needed to provide a physical framework on which to interpret single-channel data. The structure of the glutamate-gated chloride channel from *Caenorhabditis elegans* shows a much higher level of sequence identity to human hGlyR than previous templates such as AChBP or the bacterial channels, GLIC and ELIC. Thus, we constructed a model of the hGlyR and validated it against previously reported mutagenesis data. We used molecular dynamics to refine the model and to explore binding of both an agonist (glycine) and an antagonist (strychnine). The model shows excellent agreement with previous data but also suggests some unique features: (i) a water molecule that forms part of the binding site and allows us to account for some previous results that were difficult to reconcile, (ii) an interaction of the glycine agonist with S129, and (iii) an effect from E211, both of which we confirmed with new site-directed mutagenesis and patch clamp recordings. Finally, examination of the simulations suggests that strychnine binding induces movement to a conformational state distinct from the glycine-bound or apo state, not only within the ligand-binding domain but also in the transmembrane domain.

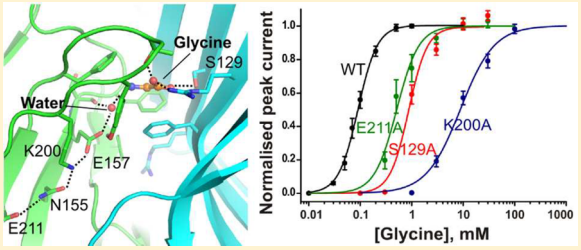

Human glycine receptors (hGlyRs) are pentameric ligand-gated ion channels (LGICs) that mediate fast inhibitory synaptic transmission in the spinal cord and brainstem.[1,2] When the neurotransmitter, glycine, binds, the hGlyRs undergo a conformational change that allows the transmembrane pore region to selectively open to permeant anions such as chloride. They are thought to play a key role in motor coordination and the processing of inflammatory pain.[3] Disruption of the normal function of hGlyRs has been linked to autism[4] and is known to cause most cases of hyperekplexia[5] (a rare inherited disease associated with an exaggerated startle response). *In vivo*, the hGlyRs can exist as homomers (comprised of only α subunits) or heteromers that contain both α and β subunits.[6] The precise combination of different subunits is spatiotemporally specific to different parts of the central nervous system (CNS).[7] *In vitro*, their suitability for single-channel work has made them a useful model for probing the energetic landscape of conformational change within ligand-gated ion channels.[8]

The hGlyRs are part of a large superfamily of receptors often termed the "Cys-loop family" of receptors,[9] which comprises both inhibitory (glycine and $GABA_A$/$GABA_C$) and excitatory (nicotinic and 5-HT_3) channels and is thus named because the extracellular domain (ECD) of each subunit contains a conserved 13-residue loop that is delimited by two cysteine residues that form a disulfide bond. For a long time, the structure of the nicotinic acetylcholine receptor[10,11] provided the only way in which to relate physiological function to a molecular framework. In recent years, however, the structural information has been extended by two main factors: (1) the discovery[12] and structural characterization of the water-soluble acetylcholine-binding proteins from four different molluscan species[13−16] and (2) the identification[17] and subsequent X-ray structures of homopentameric prokaryotic homologues.[18−20]

The acetylcholine-binding protein (AChBP) was extremely useful as a surrogate model for the binding site. Being amenable to high-resolution X-ray crystallography, AChBP clearly showed that the canonical binding sites are at the subunit interfaces and provided useful insight into the binding mode for many agonists and antagonists. In particular, AChBP structures showed how the conformation of a key loop region, loop C, varied with different compounds bound, capping the binding site more tightly when an agonist was bound. AChBP can, with some modification of the interacting loops, act as the ECD of a functional channel when fused with the transmembrane (TM)

Received: July 2, 2014
Revised: September 3, 2014
Published: September 3, 2014

domain of the $5HT_3$ receptor,[21] but AChBP structures provide no information about the channel pore or the transmembrane–ECD region interface that has to transduce the agonist binding signal to the channel gate. In addition to that, both AChBP and the prokaryotic channels are limited in their sequence identity with hGlyR α1 subunits (only 10% for AChBP). More recently, the structure of an anion-selective pentameric channel from *Caenorhabditis elegans* was determined,[22] and because it is eukaryotic and anion-selective and has the highest level of sequence identity to hGlyR α1 subunits (42%), it should provide an improved template on which to build a structural model for interpreting hGlyR single-channel data.

Despite the advances in structural information, exactly how ion channel activation maps onto the structures is still rather unclear. In particular, it remains difficult to relate observations made for AChBP and the prokaryotic LGICs to human LGICs (as recently reviewed by daCosta and Baenziger).[23] Fitting kinetic models to single-channel data from recombinant α1, α2, and $\alpha1\beta$ hGlyRs has led to the development of the so-called "flip" state model,[24−26] which incorporates shut states between agonist binding and channel opening. The "primed" states model[27] provides a similar view. The most intuitive interpretation of these models is that the closed intermediate state (flipped or primed) reflects the conformational changes in the extracellular domain before the channel opens. An ongoing goal therefore is to relate the so-called "flip state" interpreted from electrophysiological data back to structural and dynamical data at the molecular level. In the case of hGlyR, this is made more complicated by two factors. First, we do not have a crystal structure, and second, *in vivo*, the receptor can be heteromeric. Thus, for us to understand the flipped state in terms of a structure, we first have to develop a three-dimensional model that can account for existing data and make testable predictions.

Here, we report the development of a homomeric α1 model based on the recent GluCl structure and show that it has predictive power that is supported by electrophysiological experiments.

METHODS

Homology Modeling. The model of hGlyR was built using homology modeling based on methodology described previously.[28] The protein sequences of human hGlyR α1, *C. elegans* GluCl, *Gloeobacter violaceus* GLIC, *Erwinia chrysanthemi* ELIC, and human nicotinic acetylcholine receptors α1−α7, α9, and α10 were obtained from Uniprot, and a multiple-sequence alignment was generated using Muscle.[29] The sequence alignment was manually adjusted on the basis of the superimposition of the nAChR α1 [Protein Data Bank (PDB) entry 2BG9], GluCl (PDB entry 3RI5), GLIC (PDB entry 3EHZ), and ELIC (PDB entry 2VL0) structures. As the GluCl structure[22] had the highest level of sequence identity, this was chosen as the final template. The final sequence alignment between hGlyR α1 and GluCl (Figure S1 of the Supporting Information) was further edited by replacement of the gap between TM3 and TM4 of the hGlyR using a seven-residue peptide (SQPARAA) from the GLIC channel as reported previously.[30] The comparative modeling program Modeler (9v12)[31] was used to build the homology model, and 100 homology models of hGlyR were generated. The DOPE score[32] embedded in Modeler was used to rank the quality of the models. The top five hGlyR models were further evaluated using Molprobity,[33] and the top model (Figure 1) had 95% of residues in the favored region of the Ramachandran plot (Table S2 of the Supporting Information). The remaining 5% were in regions far from the binding site.

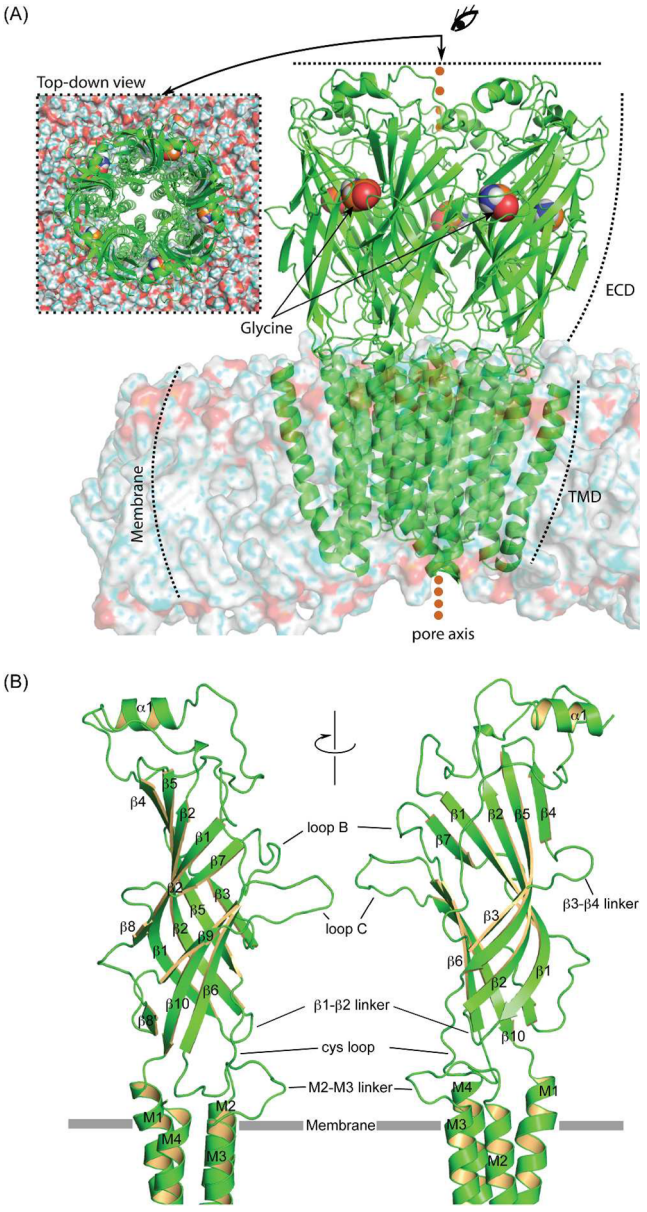

Figure 1. (A) Model of the homopentameric α1 glycine receptor (hGlyR) based on the X-ray structure of the GluCl channel from *C. elegans* (PBD entry 3RW5). Each subunit can be divided into two main domains: an extracellular domain (ECD) and a transmembrane domain (TMD). The intracellular domain is mainly comprised of the large loop between M3 and M4, which is not included in this model. The agonist glycine (spheres, not to scale) can bind to five binding sites located at the interface between adjacent subunits in the ECD. (B) Alternative views of a single subunit with the key structural features highlighted.

Initial Pose Generation. The structure of strychnine was extracted from PDB entry 2XYS.[34] Ligand docking of strychnine and glycine to the homology model was performed using AutoDock 4.2.[35] Gasteiger charges were used, and nonpolar hydrogens of the macromolecule and ligand were merged. A grid box with dimensions of 40 Å × 40 Å × 40 Å and a grid spacing of 0.375 Å was set up and centered on the "aromatic box" (residues F63, F99, F159, Y202, and F207) of

dx.doi.org/10.1021/bi500815f | *Biochemistry* 2014, 53, 6041−6051

the hGlyR model. Docking was performed using a Lamarckian genetic algorithm (LGA), with the receptor treated as rigid. For glycine, 50 complexes were generated, and the best-ranked score from the largest cluster [clustered by root-mean-square deviation (rmsd) with the threshold set at 2.0 Å] was selected as the final pose. Docking strychnine, however, was not possible via this method because the GluCl template has loop C in a "closed conformation" (because it has glutamate bound). Thus, we had to generate this initial pose manually by using the AChBP-bound pose and translating it into the hGlyR model and removing the steric clashes from loop C via steepest descent minimization.

Molecular Dynamics (MD) Simulations. MD simulations of the hGlyR in complex with glycine or strychnine (in all five binding sites) and apo were performed using Gromacs 4.6.1.[36] The homology model of the hGlyR was inserted into a pure 1-palmitoyl-2-oleoyl-*sn*-glycero-3-phosphocholine (POPC) membrane. The whole system was solvated in a box with dimensions of 130 Å × 140 Å × 140 Å containing 60769 TIP3P[37] water molecules. Na^+ and Cl^- ions were added to neutralize the system and simulate a physiological concentration of 0.15 M. The system was optimized with 2000 steps of steepest descent minimization. The temperature of the system was set to 310 K and was equilibrated for 100 ps in *NVT* and *NPT* ensembles with the protein and lipids restrained with a force of 1000 kJ mol^{-1} nm^{-2}. The restraints were removed, and the system was equilibrated for 30 ns MD in the *NPT* ensemble. During the first 10 ns of the simulation with glycine bound, we noticed that for two binding sites, a water molecule entered into the binding pocket from bulk solution and formed an interaction between the amine group of glycine and the side chain carboxyl group of E157. We repeated this process with a different force field and this time observed that a water molecule entered three of the binding sites at exactly the same position. Molecular mechanics Poisson−Boltzmann surface area (MMPB-SA) energy calculations estimate the enthalpy of glycine binding to be 4.2 ± 2.6 kcal/mol. Furthermore, docking with the water molecule present leads to only one binding mode being predicted (Figure S3 of the Supporting Information). In contrast, without water present, docking can lead to a secondary pose for glycine near the position of the proposed water. This secondary pose can also be dismissed because of its failure to account for previous mutagenesis results. Thus, we decided to include this water in all five sites for simulations of the hGlyR bound with glycine before proceeding with full production runs. This was achieved by translating the water molecule into the equivalent binding sites and fitting on the complementary subunit.

The system was equilibrated as stated before and followed by 150 ns of unrestrained MD. We set up three independent runs of five glycines bound as we noticed that in the first simulation, one of the glycines became unbound during the simulation. All the simulations were performed using the AMBER99SB-ILDN[38] force field for the lipid and protein, and the GAFF force field for the compounds with a time step of 2 fs. All bounds were restrained via the LINCS algorithm.[39] Particle mesh Ewald (PME)[40] was used with a cutoff of 10 Å for nonbonded atom interactions, and neighbor lists were updated every 10 steps. The protein, membrane, and water/ion were coupled to a temperature of 310 K with a time constant of 0.1 ps. The x and y dimensions were scaled isotropically with a Parrinello−Rahman barostat, and the z dimension was scaled independently to a reference pressure of 1 bar with a time constant of 1 ps and a compressibility of 4.5×10^{-5} bar^{-1}.

Mutations. MMPB-SA energy calculations were used to estimate the mutational energy of binding of glycine and strychnine both in the wild type (WT) and for a set of mutants within the binding site previously reported to exert an effect. Computational alanine scanning was performed with the MMPBSA.py script integrated within AMBER12. We compared these results with the effects of the same mutations on the glycine EC_{50} and the strychnine IC_{50} (measured at glycine EC_{50}) reported for recombinant glycine receptors in the literature.[41−44] We used the mutant:WT ratios of IC_{50} or EC_{50} values to estimate a free energy effect of the mutation by using $\Delta\Delta G = RT \ln(EC_{50\_mutant}/EC_{50\_WT})$ or $\Delta\Delta G = RT \ln(IC_{50\_mutant}/IC_{50\_WT})$ as appropriate.

In principle, agonist EC_{50} and antagonist IC_{50} values are affected both by binding affinity and by gating efficacy.[45] In the case of the agonist, estimating a microscopic binding affinity requires kinetic analysis of single-channel data. Our own work with this technique has allowed us to measure glycine affinity in a variety of wild-type glycine receptors, including α1 homomers. Extending this work to survey the binding site residues is not only laborious but also technically unfeasible for extreme loss-of-function mutations, where full activation can be reached only at agonist concentrations so high that they pose experimental osmotic problems.[8]

The question here is whether the functional macroscopic EC_{50} shift produced by binding site mutations can be usefully compared with the change in binding enthalpy (mutational energy) produced by simulation of the same mutations in our homology model. Given the structural data, we can safely assume that the mutations considered in Figure 5 are in the agonist-binding site and can affect agonist affinity. If a mutation affects the resting state affinity, we would expect a linear correspondence between the shift in affinity and the shift in EC_{50}. This sort of change would be seen for residues whose interaction with the agonist does not change with activation (and assumes there is no change in flipping).

We know that agonist affinity increases when the channel flips from the resting state to the preactivated intermediate, maybe because loop C closes in. It is conceivable that some mutations could reduce only this increase in affinity, by abolishing the new interactions that arise between the agonist and the protein when the receptor activates and that cause affinity to increase. For these mutations, the relation between the change in EC_{50} and the change in affinity is not straightforward. Nevertheless, we can use our single-channel data for wild-type α1 glycine receptors[24] to estimate what would happen to the glycine EC_{50} in the simplest of cases, namely if mutations eliminate the increase in agonist affinity seen with flipping. In WT channels, this is 7-fold. Because of microscopic reversibility in the allosteric mechanism, if flipping does not increase affinity, flipping cannot be favored by agonist binding and the equilibrium constants for flipping have to be the same at all states of ligation. If we assume that they are the same as the WT monoliganded flipping, the mechanism predicts that the 7-fold decrease in the affinity for the flipped state would result in a 4-fold increase in the glycine EC_{50}. Because channel opening is stabilized by the increase in the affinity in the binding site as agonists bind, these mutations are also expected to impair overall channel gating. For the mutations we examined, a substantial loss of gating (judged for instance by comparing the taurine/glycine relative maximal response) has been reported for F63A[42] (but see also ref 41) but not for F159A or R65A.

dx.doi.org/10.1021/bi500815f | *Biochemistry* 2014, 53, 6041−6051

For the antagonist, the ratio of mutant to WT IC_{50} values is expected to reflect true affinity changes produced by the mutation, in the very simplest case of mutually exclusive binding of agonist and antagonist to a single binding site and agonist responses measured without distortion by desensitization. In this case, the Cheng–Prusoff relation applies

$$K_d = \frac{IC_{50}}{1 + \frac{[A]}{EC_{50}}} \quad (1)$$

where [A] is the agonist concentration at which IC_{50} was determined. If [A] = EC_{50}, the strychnine K_d is $IC_{50}/2$. If the agonist loss of function is considerable in the mutants, EC_{50} may be too high to be measurable, because concentrations above 250–300 mM cannot be applied without increasing the solution osmolarity beyond acceptable levels. If the strychnine IC_{50} is determined against glycine concentrations below EC_{50}, the IC_{50} value would be closer to or equal to the K_d. This is the case for F63A and R65A, and this means that the experimental values we describe are lower bound estimates.

Electrophysiology. Homomeric α1 hGlyR were expressed in HEK293 cells (American Type Culture Collection) by calcium phosphate transient transfection as previously described.[46] Cells were transiently transfected with pcDNA3 plasmids (Invitrogen) encoding the α1 hGlyR subunit (GenBank accession number AJ310834) and plasmid pEGFP for the expression of the enhanced green fluorescent protein (Clontech; to allow detection of transfected cells) in a 1:2.5 ratio. The total amount of DNA was 3 μg per dish. Each dish contained 2 mL of culture medium and a single, 15 mm diameter coverslip coated with poly-L-lysine [0.1 mg/mL (Sigma)]. Dishes were 35 mm Nunc Tissue Culture dishes obtained from Scientific Laboratory Supplies (SLS). Mutations were inserted using the QuikChange site-directed mutagenesis kit (Stratagene) following the manufacturer's instructions. The full reading frame of the plasmid was sequenced by Source BioScience (http://www.lifesciences.sourcebioscience.com/).

Starting 24 h from transfection, whole-cell recording experiments were conducted at room temperature (21 °C) and a holding potential of −60 mV [uncorrected for the junction potential of 8 mV as calculated in pClamp10 (Molecular Devices)], with pipettes pulled from thick-walled borosilicate glass [with filament (Harvard Apparatus)] to a final resistance of 5–10 MΩ when filled with internal solution [consisting of 81.1 mM potassium gluconate, 11 mM EGTA, 1 mM $CaCl_2$, 1 mM $MgCl_2$, 10 mM HEPES, 20 mM TEACl, 2 mM MgATP, 40 mM glucose, and 26 mM KCl (pH adjusted to 7.4 with NaOH)]. This "low-chloride" solution was chosen for consistency with planned single-channel recordings in the cell-attached configuration, where the intracellular chloride concentration will be the physiological concentration inside a HEK cell. It is important to be consistent as intracellular chloride affects GlyR kinetics.[47] The access resistance was below 3–7 MΩ and compensated by at least 70%. The bath solution consisted of 20 mM sodium gluconate, 112.7 mM NaCl, 2 mM KCl, 2 mM $CaCl_2$, 1.2 mM $MgCl_2$, 10 mM HEPES, 10 mM TEACl, and 30 mM glucose (pH adjusted to 7.4 with NaOH). Current responses were recorded using an amplifier (AxoPatch 200B, Molecular Devices), digitized, and stored directly on a computer hard drive (sampling rate of 20 kHz, 5 kHz low-pass Bessel filter, pClamp10 software).

Different concentrations of the agonist glycine were applied for 1–2 s to cells by a U-tube,[48] achieving an exchange time of 10–50 ms. Response rundown was monitored by repeating a standard agonist concentration every fourth response and using this for compensation. Cells were discarded if rundown was >30% or if more than 15 min was needed to complete the dose–response curve.

A full concentration response curve was obtained in each cell, and peak current responses were measured and fit using CVFIT (available from OneMol.org) and the Hill equation:

$$I = I_{max}[A]^{n_H}/([A]^{n_H} + EC_{50}{}^{n_H}) \quad (2)$$

where I represents the current response, I_{max} the maximal response, A the agonist concentration, n_H the Hill coefficient, and EC_{50} the concentration of agonist needed to evoke 50% of the maximal response.

RESULTS

Conformational Behavior. Molprobity analysis of the model (Table S2 of the Supporting Information) suggested it was stereochemically sound, in fact having a percentage of residues in the favored regions higher than that in the X-ray structure of the pentameric ligand-gated ion channel of *G. violaceus*, GLIC (PDB entry 3EHZ), and the EM structure of the *Torpedo* nicotinic acetylcholine receptor (PBD entry 2BG9). We then proceeded to model agonist- and antagonist-bound states (as well as the apo receptor). To generate the initial models of the glycine (agonist)-bound and strychnine (antagonist)-bound states, we docked those ligands to all five binding sites, and given that the movement of loop C in Cys-loop receptors is thought to undergo rearrangement dependent on binding site occupancy, we performed 150 ns MD simulations to explore the binding modes further. As described in Methods, we also incorporated, into all five binding sites, a key water molecule, which in glycine-bound simulations was observed to enter the binding site directly from bulk. Because glycine is the natural agonist, we repeated that simulation two more times (giving three independent simulations in total). In one simulation, all five glycine molecules remained bound (termed the Gly5 simulation hereafter); in the second and third simulations, however, two glycines became unbound. We refer to these simulations as Gly3 and Gly3′, respectively. Analysis of Gly3 and Gly3′ simulations showed that the glycine molecules left at different times during the simulation (Figure S4 of the Supporting Information), but the pathway of dissociation was different for all four glycine molecules. Furthermore, it did not appear to correlate with large motions of loop C, though the Gly5 simulation suggests that if loop C is tightly bound, then glycine dissociation is less likely.

As a first-pass assessment of the models, the rmsd (Figure 2A) shows that there are no large conformational changes in any of the systems and that for the latter half of the simulations (75 ns onward) the trend is Apo > Stry > Gly3 > Gly3′ > Gly5, suggesting that the presence of an agonist restricts conformational movement, a feature of conformational dynamics that we have observed previously for other unrelated receptors.[49] To gain insight into which regions of the protein were differing the most between the simulations and the initial state, we performed an rmsd per residue analysis (Figure 2B). This suggests that the largest differences occur in loops A–C and also in transmembrane domains 2 and 3.

The rmsd per residue analysis (Figure 2B) suggests that the conformational variation in the strychnine and apo simulations is quite similar and is larger than that in the Gly5 simulation. The smaller change for the latter is reasonable considering the

dx.doi.org/10.1021/bi500815f | Biochemistry 2014, 53, 6041–6051

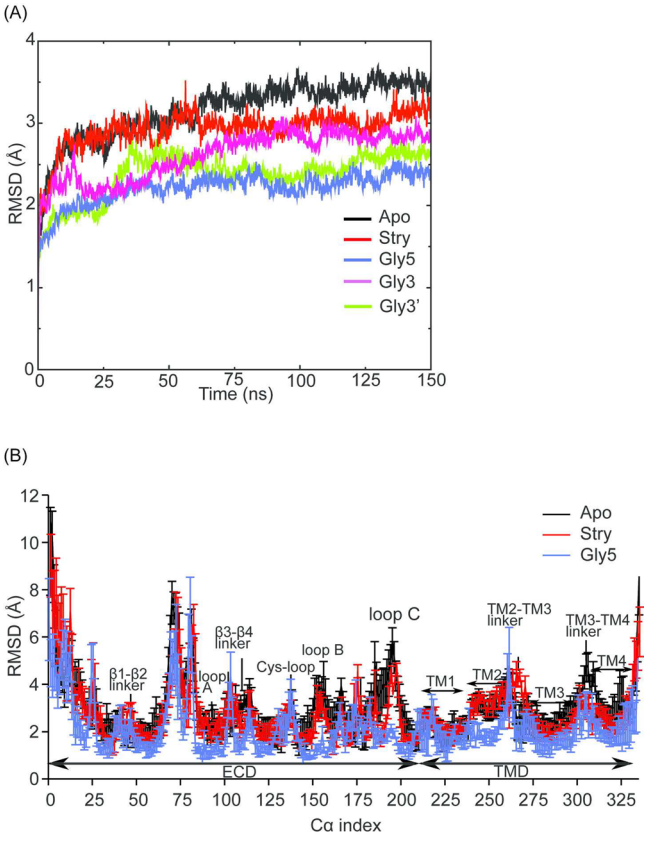

Figure 2. (A) Evolution of the Cα root-mean-square deviation (rmsd) of the human α1 glycine receptor (hGlyR) from the initial model in the MD simulations. MD simulations were performed on the hGlyR, one in the apo state (Apo), one with strychnine (Stry), and three with glycine. All binding sites were occupied at the start of the simulations. In one of the glycine-bound simulations, two glycines moved out of the binding site and three remained (Gly3); in another simulation, two glycine molecule also unbound and three remained in the binding site (Gly3′), and in the final simulation, all five glycines remained bound (Gly5). (B) Structural deviation of the hGlyR from the initial model after 150 ns as shown by the residue rmsd. The rmsd was calculated using the last frame from 150 ns of MD and the initial hGlyR model. Data for the hGlyRs in the apo state and bound with strychnine and glycine are colored black, red, and blue, respectively.

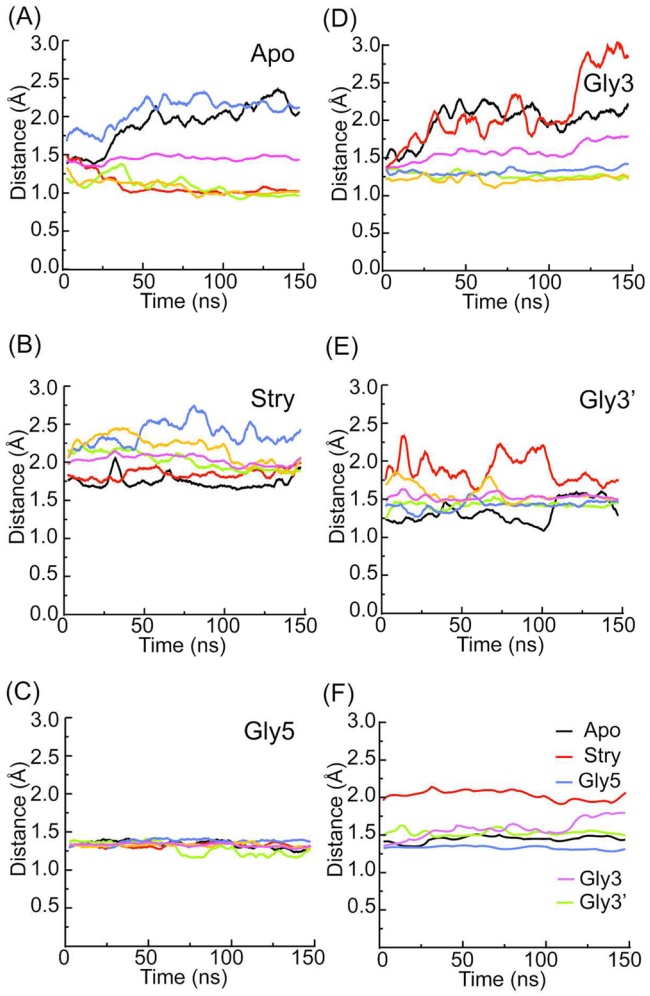

Figure 3. Loop C opening from simulations of the Apo (A), Stry (B), Gly5 (C), Gly3 (D), and Gly3′ (E) simulations defined as the distance between Cα of Q203 on loop C and Cα of S40 on the β sheet of the adjacent subunit and shown in different colors for each subunit. The mean distance is shown as the magenta line. A comparison of the mean difference between Cα of Q203 on loop C and Cα of S40 on the β sheet of the adjacent subunit obtained from each of the simulations shown in panels A–E is shown in panel F.

initial model was built using GluCl as the template and represents an open or desensitized state.[22,50] However, closer inspection revealed that the strychnine-bound simulation behaves quite differently from all the other simulations. Of central importance for Cys-loop receptor activation is the movement of loop C. We thus explored the opening and closing of loop C (Figure 3) via the definition of a distance between Cα of Q203 in loop C and Cα of S40, which is positioned on a β sheet (β1 in Figure 1B) at the rear of the binding pocket. It can be seen that the apo simulation shows (Figure 3A), as expected, considerable variation in the distance, but for the strychnine-bound simulation, the distance is at higher values consistent with the view that the presence of the antagonist prevents the full closure of loop C.[16,51]

In the glycine-bound simulations, when loop C is tightly bound, as in the Gly5 simulations (Figure 3C), glycine remains bound. From panels D and E of Figure 3, we initially suspected that loop C movement led to glycine unbinding, as in the Gly3 simulation (Figure 3E), two loops C exhibited larger distance fluctuations (red and black traces) and in the Gly3′ simulation (Figure 3D) one loop C exhibited larger distance movements (red trace). To investigate this further, we examined whether the unbinding of glycine from the principal subunit was correlated to the movement of loop C from the same subunit (Figure S4 of the Supporting Information). It appeared that there is almost no correlation between the time loop C opens (as measured by the distance between Cα of Q203 on loop C and Cα of S40 on the β sheet) and the timing of the unbinding event (as measured by the distance between the nitrogen of the glycine and Cα of F159 on the receptor). Although there was no correlation in the timing, we did observe that in three of the four simulations in which unbinding was observed, the Q203 Cα–S40 Cα distance showed a prolonged increase (reflecting opening of loop C) and that unbinding occurred during that phase of increased distance. However, we also observed that one subunit showed a prolonged increase in the Q203 Cα–S40 Cα distance, but this was not accompanied by unbinding of glycine (Figure S4B of the Supporting Information, gray traces). Thus, the opening of loop C increases the probability of glycine unbinding but does not necessarily make it inevitable on

dx.doi.org/10.1021/bi500815f | Biochemistry 2014, 53, 6041–6051

these short (150 ns) time scales. Given we also observed glycine unbinding from one subunit that showed very little increase in the Q203 Cα−S40 Cα distance, it appears that a large movement of loop C is not a prerequisite for glycine unbinding; it just appears to increase the likelihood of unbinding, as might be expected intuitively.

The GluCl structure has both an agonist and an allosteric potentiator (ivermectin) bound and has been suggested to reflect an open state.[22,52] Indeed, its minimal pore radius is 2.53 Å, which might be consistent with it being permeable to water at least in MD simulations.[52,53] However, removal of ivermectin has, in microsecond simulations, been shown to result in a closed pore conformation.[54] We analyzed the behavior of the pore region across all of the simulations and found that all of them resulted in a pore that was closed (Figure S5 of the Supporting Information), suggesting a conformational state more reflective of the desensitized state and in line with previous reports of GluCl dynamics in the absence of ivermectin,[53,54] and with models of the glycine receptor constructed from prokaryotic templates[55] and other prokaryotic LGICs.[56]

It has recently been shown that hGlyR can be made to open constitutively by inserting and cross-linking a pair of cysteines at either side of the ECD−TM domain interface. By analogy with the structure of a similarly mutated GLIC channel, it has been suggested that GlyRs can enter an "intermediate" or "locally closed" conformation[57] when a disulfide bond is formed between T54C and L274C [in the β1−β2 linker at the bottom of the ECD and in the M2−M3 linker in the TM domain (see Figure 1B)]. We explored this hypothesis in the models. We found that in the Gly5 simulation, the mean distance between T54 and L274 Cα (~5.5 Å vs 4.9 Å in ref 50) was compatible with the ability to form a disulfide bond (Figure 4). The Apo, Gly3, and Gly3′ simulations adopted positions in which the two residues were slightly further apart, but perhaps the most startling divergence was in the Stry simulation, in which this distance is increased by approximately 4 Å over the course of the simulation (Figure 4B), suggesting that the presence of an antagonist could move the receptor into a conformational state distinct from that induced by agonists from the apo conformation. Because the Gly3 and Gly3′ simulations showed glycine dissociation events, we also examined whether their timing was correlated with that of the increase in the T54 Cα−L274 Cα distance. There appeared to be no correlation between the timing of these events, but the principal subunits from which dissociation occurred were also likely to exhibit larger overall T54 Cα−L274 Cα distances. However, the small number of noisy events makes it difficult to say anything beyond speculation at this stage.

Ligand−Protein Interactions. As described in Methods, in the initial MD runs of the apoprotein, we observed a water enter the binding pocket and occupy a position near the side chain carboxyl oxygens of E157. Two or three (we repeated the simulations) water molecules were seen to enter in <10 ns, suggesting that this position is favorable for water occupancy, and thus, this water was included in all glycine-bound simulations, where it was observed to be maintained in all binding sites for the whole duration of the simulations. When the glycine is bound, the water essentially mediates the contact of the amine group of the glycine with E157 (Figure 5A). The water molecule is additionally stabilized by contacts with S158. This differs from the previously proposed model of Grudzinska et al.[41] in which the glycine interacts directly with E157, with

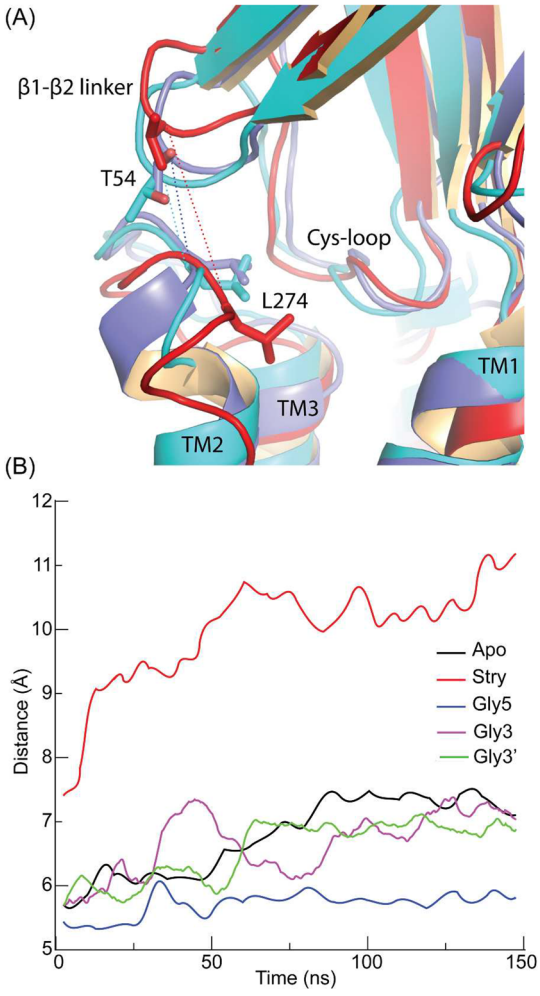

Figure 4. Analysis suggests that the conformational state of the glycine-bound and Stry simulations may reflect the recently identified locally closed state. (A) Overlay of the initial model (cyan), the Gly5 final frame at 150 ns (purple), and the Stry final snapshot (red) showing the relative positions of T54 and L274 that Prevost et al. recently showed that when mutated to cysteine and oxidized could form a locally closed state. (B) Evolution of the T54 Cα−L274 Cα distance as a function of time. It is apparent that the strychnine-bound state is conformationally distinct and places these residues at a distance that is not compatible with disulfide bond formation.

no water in the binding site. Our model is consistent with the data and the model of Pless et al.[58] in that there is an interaction with F159, although not as strong (on the simple basis of distance) as might be expected from their interpretation, and that there is not a cation−π interaction of the glycine amino moiety with F207. The carboxyl end of glycine is stabilized by S129 and R65. The mode of interaction with strychnine bound (Figure 5B) shows that the antagonist pushes loop C outward and forms many nonpolar interactions, with F63, F159, and Y202 in particular.

As a step toward validating the model, we estimated the energetic contribution to binding of several mutations predicted by the model with glycine or strychnine bound using an MMPB-SA approach (see Methods). When compared to a simple model to account for EC_{50} or IC_{50} changes (see Methods), the predicted effects on the binding affinity are in remarkably good agreement with IC_{50} data for these residues in

dx.doi.org/10.1021/bi500815f | Biochemistry 2014, 53, 6041−6051

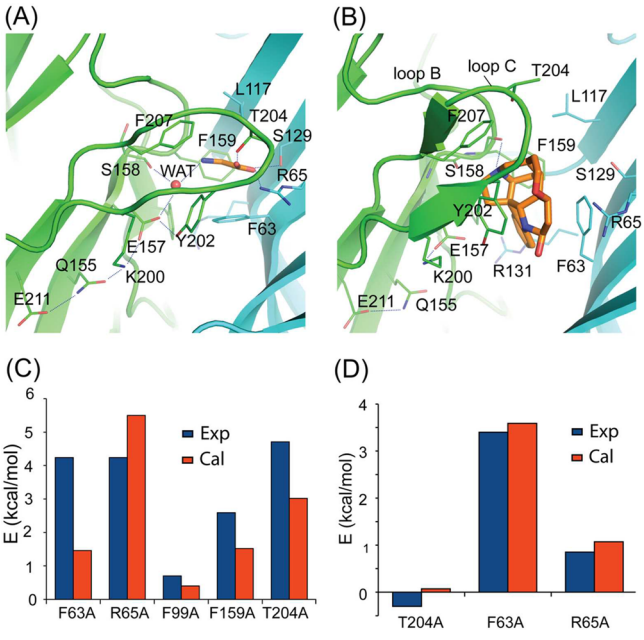

Figure 5. Binding modes of glycine (A) and strychnine (B). The principal subunit, the complementary subunit, and the ligands are colored green, light blue, and orange, respectively. The water molecule found to enter the binding pocket to help stabilize the bound glycine is shown as a red sphere and labeled WAT. A hydrogen bond network among E211, Q155, K200, and E157 is shown using blue dashed lines. Panels C and D show the mutational energies, which were derived from experimental data,[41,44] via the use of $\Delta\Delta G = RT \ln(EC_{50\_mutant}/EC_{50\_WT})$ or $\Delta\Delta G = RT \ln(IC_{50\_mutant}/IC_{50\_WT})$ as appropriate (blue bars; see Methods for assumptions), and calculated using the MM-PBSA method (red bars). Given the profound loss of agonist potency for F63A and R65A (see Methods), the blue bars are a lower bound value. Upper bounds are 3.79 and 1.276 kcal/mol for F63A and R65A, respectively.

the binding site[41,44] as can be seen in panels C and D of Figure 5.

Because the interaction of E157 with the water is a feature unique to our model, we explored the effect of mutating this residue to aspartate via additional 100 ns simulations. The E157D mutation maintains the negative charge but decreases the length of the side chain. We hypothesized that the shorter side chain should be less effective at stabilizing the intermediate water molecule. As expected, we observed that this water molecule in the mutant exchanged much more readily with bulk water molecules than the wild type did (Figure 6). Furthermore, the carboxylate oxygen in D157 in the mutant is much less able to make a hydrogen bond with the Y202 hydroxyl side chain, and this results in a more mobile loop C even in the presence of the agonist (Figure 6D,E). Experimentally, Betz and co-workers[41] showed that the E157D mutant exhibits a dramatic increase in the glycine EC_{50}, which they interpreted as the weakening of a direct interaction between residue 157 and the glycine molecule. In our model, the glycine is shifted more toward the complementary subunit (on the right-hand side of Figure 6), and a consequence of that is that it also interacts with a previously unreported (in glycine receptors) residue, S129. Interestingly, when the equivalent position in nicotinic acetylcholine receptors was mutated to a cysteine along with another cysteine in loop C, oxidizing conditions led to channels that exhibited long openings in quick succession, suggesting that a covalent trapping of the conformation of loop C leads to a higher likelihood of being in the flipped (primed) state.[27] To test our model further, we introduced an S129A mutation and obtained a dose–response curve for glycine on the homomeric mutant receptor by whole-cell patch clamp. Figure 7 shows the normalized current response and clearly shows that that S129A mutation decreases the potency of glycine and causes a rightward shift in EC_{50} from 0.1 to 0.9 mM, thus validating the mode of glycine binding shown by our model.

DISCUSSION

Previous models of hGlyRs were mostly based on the acetylcholine-binding protein or the GLIC channel from *G. violaceus*. The GluCl channel shows a much higher level of sequence identity and is also anion-selective. Thus, it may be a more suitable template for the generation of a model in the absence of a crystal structure for hGlyR itself. James et al.[59] recently used GluCl as a template for their human hGlyR model, but with a view of examining mutations in the transmembrane domain, rather than in the ligand-binding region as we do here. One notable difference in our model compared to previous models was the consideration of a potential water molecule in the binding site. There is growing recognition of the importance of water in the ligand binding process,[60,61] and indeed, in the related acetylcholine-binding protein (AChBP) crystal structures (which are sometimes used as a surrogate for full-length nicotinic acetylcholine receptors), water molecules have been observed to mediate ligand–protein interactions.[13,15,62] Thus, there is a structural precedent for modeling a water molecule within this pocket. The location of this water leads to an important difference between our and previously reported ligand-binding site models of the hGlyR.

Grudzinska et al.[41] argued that a direct interaction between the amino group of glycine and E157 was likely on the basis of the dramatic increase in the EC_{50} for glycine produced by the E157D mutation. The relative decrease in the potency of taurine was represented to be smaller, which was rationalized on the basis that taurine is longer and thus could "extend" far enough to reach the shorter aspartic acid in the E157D mutant. However, the absolute EC_{50} values for glycine and taurine could not be reliably measured in the mutant, where they are equal to or greater than 250 and 300 mM, respectively, indicating substantial but indistinguishable loss of potency for both agonists. Therefore, it is not entirely obvious this model accounts for the mutational effects completely. Our model and simulation data provide an alternative explanation for the change in efficacy in the E157D mutant. In our model, we noticed that there was an extensive hydrogen bonding network that links the agonist through a water molecule to E157 to K200 to Q155 to E211 (see Figure 5A). In the E157D simulations (Figure 6), we observed that the water molecule was rather less stable than that in WT simulations, thus interrupting the hydrogen bonding network in this region. This also disrupts the interaction between the side chain at 157 and Y202, which in turn leads to an increased level of movement of loop C, even on the time scale of these simulations.

To explore this hypothesis further, we introduced K200A and E211A mutations and found that E211A produces a modest increase in glycine EC_{50}, comparable to that seen with S129A [0.51 ± 0.13 and 0.90 ± 0.31 mM (n = 4 and 5) for E211A and S129A, respectively, vs 0.10 ± 0.01 mM in WT (n = 7)]. A greater loss of glycine sensitivity was seen with K200A, which had an EC_{50} of 8.75 ± 1.8 mM (n = 4), in agreement with the

dx.doi.org/10.1021/bi500815f | *Biochemistry* 2014, 53, 6041–6051

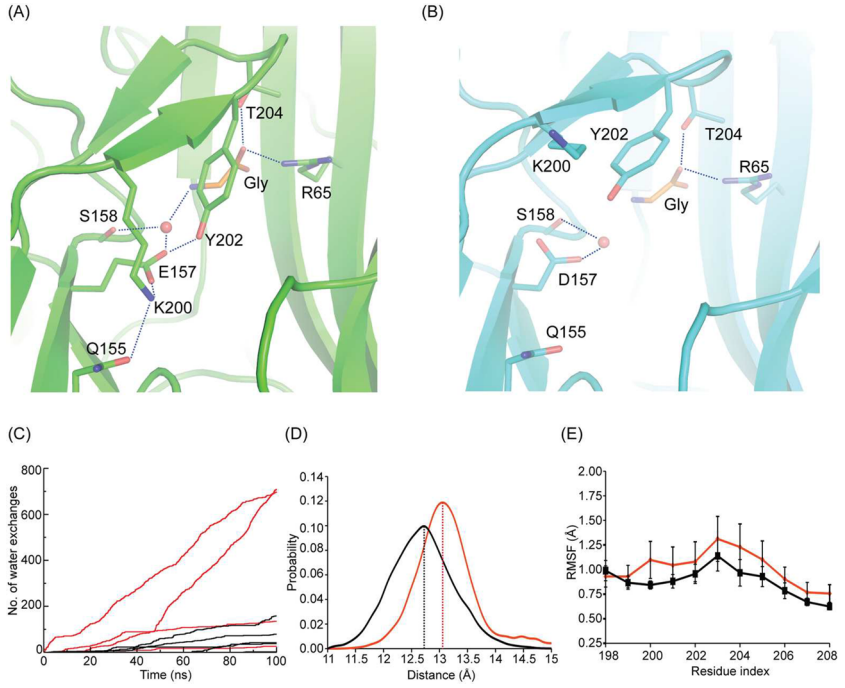

Figure 6. Mutational effect of the E157D mutation. (A) WT, in which E157 participates in an extensive hydrogen bonding network. (B) In the E157D mutation, this network is destroyed and the amino group of the agonist often fails to make a hydrogen bond with the water, which in turn is destabilized. (C) Number of water exchanges at this position vs time for WT (black) and the E157D mutant (red). The water at two of the binding pockets undergoes substantial exchange. There are only four lines because one glycine left the binding pocket in these simulations. (D) Distribution of the distance between Cα of E157 and Cα of Y202 of the five binding sites. (E) Root-mean-square fluctuations of loop C residues.

report by Rajendra et al.[63] Although this correlation is alluring, we should note that this requires much more detailed examination as one always has to be careful when relating EC_{50} data back to a physical model of interactions, and it is impossible to tell at this stage whether the mutation disrupts the initial binding of glycine to the resting state, the glycine stabilization of the preopening intermediate state, or the ability of glycine to open the channel once bound (for a discussion, see Methods). One interpretation is that our model suggests that this hydrogen bonding network may play an important role in transmitting the effect of glycine binding down to the transmembrane domain and that interference of this network will lead to changes in the EC_{50}. However, we cannot rule out alternative explanations; this hydrogen bonding network could have a purely local effect as a means of optimizing ligand binding, for example.

Even though the binding mode reported by Pless et al. does not involve a water molecule, the pose is in fact quite close to that presented here, although our initial pose does not place the amine group as close to F159 as they have. The binding pose in their paper[58] was based on the interpretation of cation$-\pi$ effects whereby there was a clear correlation between the glycine EC_{50} and the cation$-\pi$ binding ability of the fluorinated Phe derivatives at position 159, but not at other positions. In the simulations, the amine group of the glycine can get close to F159 and is typically between 3.5 and 4 Å away. Modern force fields do not explicitly account for cation$-\pi$ interactions. Overall though, these poses are in reasonable agreement.

An added complication to this analysis was that the glycine molecules were prone to unbinding. Interestingly, there was no obvious correlation between the extent of loop C opening and the dissociation of glycine, and indeed, we observed different pathways for each dissociation event. It appears that only a small movement of loop C is required to allow the glycine to escape (see Figure 3). It is tempting to speculate here that loop C has to fully lock down before that subunit can contribute to the activation process, and that this motion might form a component at least of the flipped state. Furthermore, even in the Gly5 simulations, the mobility of the glycine ligands was very dynamic within the binding pocket. This might appear to be counterintuitive given that glycine is the endogenous ligand. However, it may well reflect the fact glycine can adopt many different orientations while bound to the receptor, but that only one binding mode is compatible with entering the flipped state.

Conformational State. During the simulations reported here, the model was observed to undergo a distinct closing in the TM region. Closing of the pore was observed previously in simulations of GluCl.[53] In that study, they speculated the closure could be attributed to the absence of ivermectin or due to an intrinsic closing tendency, which had also been postulated for simulations of the GLIC channel.[64] More recently, simulations of GluCl with and without ivermectin present[54] confirmed the apparent role of this molecule in affording stabilization of a more open conformation. Ivermectin is known to interact with hGlyRs,[65] so it would seem likely the behavior of the TM is a reflection of its similarity to the GluCl channel. Indeed, preliminary simulations with ivermectin to our model suggest it is capable of maintaining the open state of the channel.

However, what was particularly striking was the observation that the state of the strychnine-bound simulation (Stry), although also closed, appears to be very different in terms of the LBD−TM interface gating region. The glycine-bound and apo simulations appear to reflect the locally closed state as recently proposed for hGlyR,[57] but the strychnine-bound simulation appears to be much more strongly influenced by the presence

dx.doi.org/10.1021/bi500815f | *Biochemistry* 2014, 53, 6041−6051

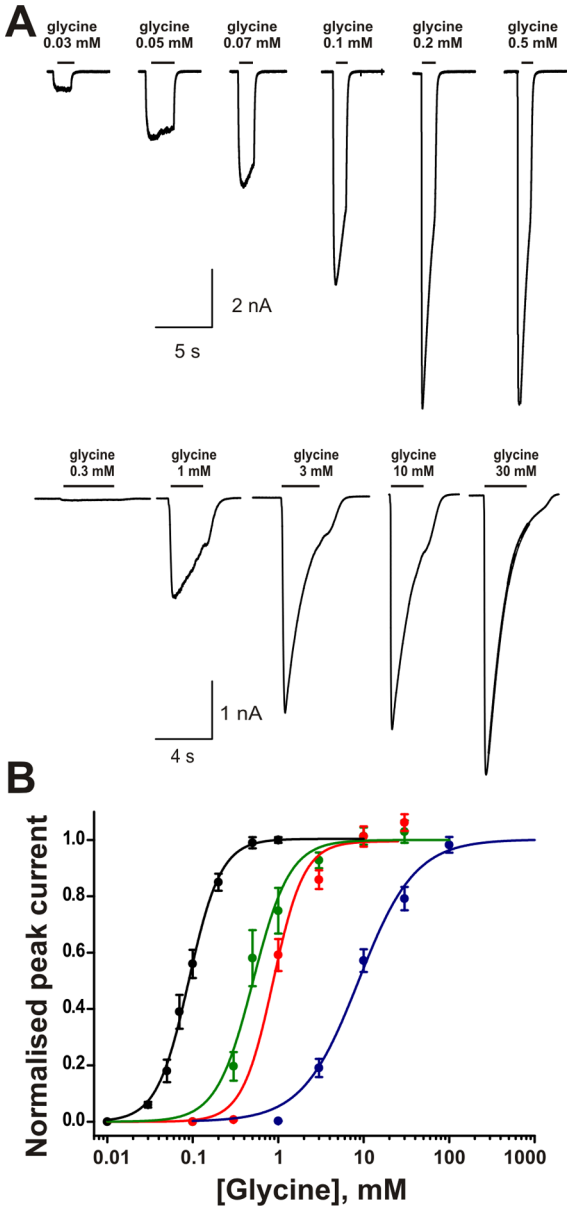

Figure 7. Sensitivity of the channel to the agonist glycine is reduced by mutating residues predicted to interact directly with the agonist (S129) or indirectly via the hydrogen bond network shown in Figure 5 (K200 and E211). (A) Whole-cell current responses recorded for WT (top) and S129A mutant (bottom) hGlyRs in response to the application of various concentrations of glycine. (B) Dose−response curves for hGlyRs, normalized to their maximal response: WT (black), S129A (red), E211A (green), and K200A (blue). The symbols show the mean values (with error bars for the standard deviation of the mean, where this is larger than the symbol size) for the recordings included in the analysis (n = 4−7 cells). The solid lines are fits of the Hill equation.

of the antagonist. This suggests that the effect of the antagonist on the loop C conformation is transmitted more immediately to the LBD−TM interface. Fluorimetry experiments have previously suggested that strychnine or other competitive antagonists can induce distinct conformational changes (compared to agonist-bound protein or apoprotein) in Cys-loop receptors, as exemplified in both $GABA_A$ receptors[66] and hGlyR.[67,68]

Clearly though, more repeats of this setup would be beneficial for determining whether this effect is a genuine consequence of antagonist binding or just a stochastic process at this stage. That is beyond scope of this work but is something we are currently exploring further. Determining the mechanistic state to which the physical models correspond has proven to be more difficult than anticipated, and it may well be that there are subtle, but distinct, differences between prokaryotes and eukaryotes adding to the complication.[23] Regardless, when compared to the recent nuclear magnetic resonance structure of the transmembrane domain,[69] the pore region is most definitely closed in all of our systems.

CONCLUSION

We have shown here that the GluCl structure can provide a good template for modeling the human hGlyR α1 homopentamer. The model suggested the inclusion of a key water molecule in the binding pocket and allowed us to make prospective predictions that have allowed us to identify another residue, S129, that plays a central role in agonist binding. For the agonist-bound form and the apo state, we suggest the model most closely resembles the locally closed state, but for strychnine, it may be more reflective of the resting state of the receptor.

ASSOCIATED CONTENT

Supporting Information

Sequence alignments, model quality assessment data, and additional figures. This material is available free of charge via the Internet at http://pubs.acs.org.

AUTHOR INFORMATION

Corresponding Authors

*E-mail: l.sivilotti@ucl.ac.uk.

*E-mail: philip.biggin@bioch.ox.ac.uk Telephone: +44 1865 613305. Fax: +44 1865 613238.

Funding

This work was supported by MRC Grant MR/J007110/1.

Notes

The authors declare no competing financial interest.

ACKNOWLEDGMENTS

We thank the Advanced Research Computing centre for computer time.

REFERENCES

(1) Legendre, P. (2001) The glycinergic inhibitory response. *Cell. Mol. Life Sci. 58*, 760−793.

(2) Lynch, J. W. (2004) Molecular structure and function of the glycine receptor chloride channel. *Physiol. Rev. 84*, 1051−1095.

(3) Lynch, J., and Callister, R. (2006) Glycine receptors: A new therapeutic target in pain pathways. *Curr. Opin. Invest. Drugs 7*, 48−53.

(4) Piton, A., Gauthier, J., Hamdan, F. F., Lafreniere, R. G., Yang, Y., Henrion, E., Laurent, S., Noreau, A., Thibodeau, P., Karemera, L., Spiegelman, D., Kuku, F., Duguay, J., Destroismaisons, L., Jolivet, P., Cote, M., Lachapelle, K., Diallo, O., Raymond, A., Marineau, C., Champagne, N., Xiong, L., Gaspar, C., Riviere, J. B., Tarabeux, J., Cossette, P., Krebs, M. O., Rapoport, J. L., Addington, A., DeLisi, L. E., Mottron, L., Joober, R., Fombonne, E., Drapeau, P., and Rouleau, G. A. (2011) Systematic resequencing of X-chromosome synaptic genes in autism spectrum disorder and schizophrenia. *Mol. Psychiatry 16*, 867−880.

(5) Bode, A., and Lynch, J. (2014) The impact of human hyperekplexia mutations on glycine receptor structure and function. *Mol. Brain 7*, 2.
(6) Langosch, D., Thomas, L., and Betz, H. (1988) Conserved quaternary structure of ligand-gated ion channels: The postsynaptic glycine receptor is a pentamer. *Proc. Natl. Acad. Sci. U.S.A. 85*, 7394−7398.
(7) Watanabe, E., and Akagi, H. (1995) Distribution patterns of mRNAs encoding glycine receptor channels in the developing rat spinal cord. *Neurosci. Res. 23*, 377−382.
(8) Sivilotti, L. G. (2010) What single-channel analysis tells us of the activation mechanism of ligand-gated channels: The case of the glycine receptor. *J. Physiol. 588*, 45−58.
(9) Schofield, P. R., Darlison, M. G., Fujita, N., Burt, D. R., Stephenson, F. A., Rodriguez, H., Rhee, L. M., Ramachandran, J., Reale, V., Glencorse, T. A., Seeburg, P. H., and Barnard, E. A. (1987) Sequence and functional expression of the $GABA_A$ receptor shows a ligand gated receptor super family. *Nature 328*, 221−227.
(10) Unwin, N. (1995) Acetylcholine receptor channel imaged in the open state. *Nature 373*, 37−43.
(11) Unwin, N. (2005) Refined structure of the nicotinic acetylcholine receptor at 4 Å resolution. *J. Mol. Biol. 346*, 967−989.
(12) Smit, A. B., Syed, N. I., Schaap, D., van Minnen, J., Klumperman, J., Kits, K. S., Lodder, H., van der Schors, R. C. v., van Elk, R., Sorgedrager, B., Brejc, K., Sixma, T. K., and Geraerts, W. P. (2001) A glia-derived acetylcholine-binding protein that modulates synpatic transmission. *Nature 411*, 261−268.
(13) Billen, B., Spurny, R., Brams, M., van Elk, R., Valera-Kummer, S., Yakel, J. L., Voets, T., Bertrand, D., Smit, A. B., and Ulens, C. (2012) Molecular actions of smoking cessation drugs at $\alpha4\beta2$ nicotinic receptors defined in crystal structures of a homologous binding protein. *Proc. Natl. Acad. Sci. U.S.A. 109*, 9173−9178.
(14) Brejc, K., van Dijk, W. J., Klassen, R. V., Schuurmans, M., van Der Oost, J., Smit, A. B., and Sixma, T. K. (2001) Crystal structure of an ACh-binding protein reveals the ligand-binding domain of nicotinic receptors. *Nature 411*, 269−276.
(15) Celie, P. H., van Rossum-Fikkert, S. H., van Dijk, W. J., Brejc, K., Smit, A. B., and Sixma, T. K. (2004) Nicotine and carbamylcholine binding to nicotinic acetylcholine receptors as studied in AChBP crystal structures. *Neuron 41*, 907−914.
(16) Hansen, S. B., Sulzenbacher, G., Huxford, T., Marchot, P., Taylor, P., and Bourne, Y. (2005) Structures of the *Aplysia* AChBP complexes with nicotinic agonists and antagonists reveal distinctive binding interfaces and conformations. *EMBO J.*, 1−12.
(17) Tasneem, A., Iyer, L., Jakobsson, E., and Aravind, L. (2005) Identification of the prokaryotic ligand-gated ion channels and their implications for the mechanisms and origins of animal Cys-loop ion channels. *Genome Biol. 6*, R4.
(18) Bocquet, N., Nury, H., Baaden, M., Le Poupon, C., Changeux, J.-P., Delarue, M., and Corringer, P.-J. (2009) X-ray structure of a pentameric ligand-gated ion channel in an apparently open conformation. *Nature 457*, 111−114.
(19) Hilf, R. J. C., and Dutzler, R. (2008) X-ray structure of a prokaryotic pentameric ligand-gated ion channel. *Nature 452*, 375−379.
(20) Hilf, R. J. C., and Dutzler, R. (2009) Structure of a potentially open state of a proton-activated pentameric ligand-gated ion channel. *Nature 457*, 115−118.
(21) Bouzat, C., Gumilar, F., Spitzmaul, G., Wang, H. L., Rayes, D., Hansen, S. B., Taylor, P., and Sine, S. M. (2004) Coupling of agonist binding to channel gating in an ACh-binding protein linked to an ion channel. *Nature 430*, 269−276.
(22) Hibbs, R., and Gouaux, E. (2011) Principles of activation and permeation in an anion-selective Cys-loop receptor. *Nature 474*, 54−60.
(23) daCosta, C. J. B., and Baenziger, J. E. (2013) Gating of pentameric ligand-gated ion channels: Structural insights and ambiguities. *Structure 21*, 1271−1283.
(24) Burzomato, V., Beato, M., Groot-Kormelink, P. J., Colquhoun, D., and Sivilotti, L. G. (2004) Single-channel behavior of heteromeric $\alpha1\beta$ glycine receptors: An attempt to detect a conformational change before the channel opens. *J. Neurosci. 24*, 10924−10940.
(25) Krashia, P., Lape, R., Lodesani, F., Colquhoun, D., and Sivilotti, L. G. (2011) The long activations of $\alpha2$ glycine channels can be described by a mechanism with reaction intermediates ("flip"). *J. Gen. Physiol. 137*, 197−216.
(26) Lape, R., Colquhoun, D., and Sivilotti, L. G. (2008) On the nature of partial agonism in the nicotinic receptor superfamily. *Nature 454*, 722−727.
(27) Mukhtasimova, N., Lee, W. Y., Wang, H.-L., and Sine, S. M. (2009) Detection and trapping of intermediate states priming nicotinic receptor channel opening. *Nature 459*, 451−454.
(28) Yu, R., Craik, D. J., and Kaas, Q. (2011) Blockade of neuronal $\alpha7$-nAChR by α-conotoxin ImI explained by computational scanning and energy calculations. *PLoS Comput. Biol. 7*, e1002011.
(29) Edgar, R. C. (2004) MUSCLE: A multiple sequence alignment method with reduced time and space complexity. *BMC Bioinf. 5*, 113.
(30) Moroni, M., Biro, I., Giugliano, M., Vijayan, R., Biggin, P. C., Beato, M., and Svililotti, L. (2011) Chloride ions in the pore of Gly and GABA channels shape the time course and voltage dependence of agonist currents. *J. Neurosci. 31*, 14095−14106.
(31) Eswar, N., Webb, B., Marti-Renom, M. A., Madhusudhan, M. S., Eramian, D., Shen, M.-y., Pieper, U., and Sali, A. (2006) Comparative protein structure modeling using Modeller. In *Current Protocols in Bioinformatics*, John Wiley & Sons, Inc., New York.
(32) Shen, M.-Y., and Sali, A. (2006) Statistical potential for assessment and prediction of protein structures. *Protein Sci. 15*, 2507−2524.
(33) Davis, I. W., Leaver-Fay, A., Chen, V. B., Block, J. N., Kapral, G. J., Wang, X., Murray, L. W., Arendall, W. B., Snoeyink, J., Richardson, J. S., and Richardson, D. C. (2007) MolProbity: All-atom contacts and structure validation for proteins and nucleic acids. *Nucleic Acids Res. 35*, W375−W383.
(34) Brams, M., Pandya, A., Kuzmin, D., van Elk, R., Krijnen, L., Yakel, J. L., Tsetlin, V., Smit, A. B., and Ulens, C. (2011) A structural and mutagenic blueprint for molecular recognition of strychnine and *d*-tubocurarine by different cys-loop receptors. *PLoS Biol. 9*, e1001034.
(35) Morris, G. M., Huey, R., Lindstrom, W., Sanner, M. F., Belew, R. K., Goodsell, D. S., and Olson, A. J. (2009) AutoDock 4 and AutoDockTools 4: Automated docking with selective receptor flexibility. *J. Comput. Chem. 30*, 2785−2791.
(36) Pronk, S., Páll, S., Schulz, R., Larsson, P., Bjelkmar, P., Apostolov, R., Shirts, M. R., Smith, J. C., Kasson, P. M., van der Spoel, D., Hess, B., and Lindahl, E. (2013) GROMACS 4.5: A high-throughput and highly parallel open source molecular simulation toolkit. *Bioinformatics 29*, 845−854.
(37) Jorgensen, W. L. (1981) Transferable intermolecular potential functions for water, alcohols, and ethers, application to liquid water. *J. Am. Chem. Soc. 103*, 335−340.
(38) Lindorff-Larsen, K., Piana, S., Palmo, K., Maragakis, P., Klepeis, J., Dror, R., and Shaw, D. (2010) Improved side-chain torsion potentials for the Amber ff99SB protein force field. *Proteins: Struct., Funct., Genet. 78*, 1950−1958.
(39) Hess, B., Bekker, H., Berendsen, H. J. C., and Fraaije, J. G. E. M. (1997) LINCS: A Linear Constraint Solver for Molecular Simulations. *J. Comput. Chem. 18*, 1463−1472.
(40) Darden, T., York, D., and Pedersen, L. (1993) Particle mesh Ewald: An N.log(N) method for Ewald sums in large systems. *J. Chem. Phys. 98*, 10089−10092.
(41) Grudzinska, J., Schemm, R., Haeger, S., Nicke, A., Schmalzing, G., Betz, H., and Laube, B. (2005) The β subunit determines the ligand binding properties of synaptic glycine receptors. *Neuron 45*, 727−739.
(42) Pless, S. A., Hanek, A. P., Price, K. L., Lynch, J. W., Lester, H. A., Dougherty, D. A., and Lummis, S. C. R. (2011) A cation-π interaction at a phenylalanine residue in the glycine receptor binding site is conserved for different agonists. *Mol. Pharmacol. 79*, 742−748.

(43) Vafa, B., Lewis, T. M., Cunningham, A. M., Jacques, P., Lynch, J. W., and Schofield, P. R. (1999) Identification of a new ligand binding domain in the α1 subunit of the inhibitory glycine receptor. *J. Neurochem. 73*, 2158−2166.
(44) Vandenberg, R. J., Handford, C. A., and Schofield, P. R. (1992) Distinct agonist- and antagonist-binding sites on the glycine receptor. *Neuron 9*, 491−496.
(45) Colquhoun, D. (1998) Binding, gating, affinity and efficacy: The interpretation of structure-activity relationships for agonists and of the effects of mutating receptors. *Br. J. Pharmacol. 125*, 923−947.
(46) Groot-Kormelink, P. J., Beato, M., Finotti, C., Harvey, R. J., and Sivilotti, L. G. (2002) Achieving optimal expression for single channel recording: A plasmid ratio approach to the expression of α1 glycine receptors in HEK293 cells. *J. Neurosci. Methods 113*, 207−214.
(47) Pitt, S. J., Sivilotti, L. G., and Beato, M. (2008) High intracellular chloride slows the decay of glycinergic currents. *J. Neurosci. 28*, 11454−11467.
(48) Krishtal, O. A., and Pidoplichko, V. I. (1980) A receptor for protons in the nerve cell membrane. *Neuroscience 5*, 2325−2327.
(49) Arinaminpathy, Y., Sansom, M. S. P., and Biggin, P. C. (2002) Molecular dynamics simulations of the ligand-binding domain of the ionotropic glutamate receptor GluR2. *Biophys. J. 82*, 676−683.
(50) Akabas, M. H. (2013) Using molecular dynamics to elucidate the structural basis for function in pLGICs. *Proc. Natl. Acad. Sci. U.S.A. 110*, 16700−16701.
(51) Celie, P. H., Kasheveroc, I. E., Mordvintsev, D. Y., Hogg, R. C., van Nierop, P., van Elk, R., van Rossum-Fikkert, S. H., Zhmak, M. N., Bertrand, D., Tsetlin, V., Sixma, T. K., and Smit, A. B. (2005) Crystal structure of nicotinic acetylcholine receptor homolog AChBP in complex with an α-conotoxin PnIA variant. *Nat. Struct. Mol. Biol. 12*, 582−588.
(52) Calimet, N., Simoes, M., Changeux, J.-P., Karplus, M., Taly, A., and Cecchini, M. (2013) A gating mechanism of pentameric ligand-gated ion channels. *Proc. Natl. Acad. Sci. U.S.A. 110*, E3987−E3996.
(53) Cheng, M. H., and Coalson, R. D. (2012) Energetics and ion permeation characteristics in a glutamate-gated chloride (GluCl) receptor channel. *J. Phys. Chem. B 116*, 13637−13643.
(54) Yoluk, Ö., Brömstrup, T., Bertaccini, E. J., Trudell, J. R., and Lindahl, E. (2013) Stabilization of the GluCl ligand-gated ion channel in the presence and absence of ivermectin. *Biophys. J. 105*, 640−647.
(55) Murail, S., Wallner, B., Trudell, J. R., Bertaccini, E., and Lindahl, E. (2011) Microsecond simulations indicate that ethanol binds between subunits and could stabilize an open-state model of a glycine receptor. *Biophys. J. 100*, 1642−1650.
(56) LeBard, D. N., Hénin, J., Eckenhoff, R. G., Klein, M. L., and Brannigan, G. (2012) General anesthetics predicted to block the GLIC pore with micromolar affinity. *PLoS Comput. Biol. 8*, e1002532.
(57) Prevost, M. S., Moraga-Cid, G., Van Renterghem, C., Edelstein, S. J., Changeux, J.-P., and Corringer, P.-J. (2013) Intermediate closed state for glycine receptor function revealed by cysteine cross-linking. *Proc. Natl. Acad. Sci. U.S.A. 110*, 17113−17118.
(58) Pless, S. A., Millen, K. S., Hanek, A. P., Lynch, J. W., Lester, H. A., Lummis, S. C. R., and Dougherty, D. A. (2008) A cation-π interaction in the binding site of the glycine receptor is mediated by a phenylalanine residue. *J. Neurosci. 28*, 10937−10942.
(59) James, V. M., Bode, A., Chung, S.-K., Gill, J. L., Nielsen, M., Cowan, F. M., Vujic, M., Thomas, R. H., Rees, M. I., Harvey, K., Keramidas, A., Topf, M., Ginjaar, I., Lynch, J. W., and Harvey, R. J. (2013) Novel missense mutations in the glycine receptor β subunit gene (GLRB) in startle disease. *Neurobiol. Dis. 52*, 137−149.
(60) Lu, Y., Wang, R., Yang, C.-Y., and Wang, S. (2007) Analysis of ligand-bound water molecules in high resolution crystal structures of protein-ligand complexes. *J. Chem. Inf. Model. 47*, 668−675.
(61) Ross, G. A., Morris, G. M., and Biggin, P. C. (2012) Rapid and Accurate Prediction and Scoring of Water Molecules in Protein Binding Sites. *PLoS One 7*, e32036.
(62) Zhang, H.-K., Eaton, J. B., Yu, L.-F., Nys, M., Mazzolari, A., van Elk, R., Smit, A. B., Alexandrov, V., Hanania, T., Sabath, E., Fedolak, A., Brunner, D., Lukas, R. J., Vistoli, G., Ulens, C., and Kozikowski, A. P. (2012) Insights into the structural determinants required for high-affinity binding of chiral cyclopropane-containing ligands to $\alpha4\beta2$-nicotinic acetylcholine receptors: An integrated approach to behaviorally active nicotinic ligands. *J. Med. Chem. 55*, 8028−8037.
(63) Rajendra, S., Vandenberg, R. J., Pierce, K. D., Cunningham, A. M., French, P. W., Barry, P. H., and Schofield, P. R. (1995) The unique extracellular disulfide loop of the glycine receptor is a principal ligand binding element. *EMBO J. 14*, 2987−2998.
(64) Willenbring, D., Liu, Lu. T., Mowrey, D., Xu, Y., and Tang, P. (2011) Isoflurane alters the structure and dynamics of GLIC. *Biophys. J. 101*, 1905−1912.
(65) Lynagh, T., and Lynch, J. (2012) Molecular mechanisms of Cys-loop ion channel receptor modulation by ivermectin. *Front. Mol. Neurosci. 5*, 60.
(66) Chang, Y., and Weiss, D. S. (2002) Site-specific fluorescence reveals distinct structural changes with GABA receptor activation and antagonism. *Nat. Neurosci. 5*, 1163−1168.
(67) Pless, S. A., and Lynch, J. W. (2009) Ligand-specific conformational changes in the α1 glycine receptor ligand-binding domain. *J. Biol. Chem. 284*, 15847−15856.
(68) Talwar, S., Lynch, J. W., and Gilbert, D. F. (2013) Fluorescence-based high-throughput functional profiling of ligand-gated ion channels at the level of single cells. *PLoS One 8*, e58479.
(69) Mowrey, D. D., Cui, T., Jia, Y., Ma, D., Makhov, A. M., Zhang, P., Tang, P., and Xu, Y. (2013) Open-Channel Structures of the Human Glycine Receptor α1 Full-Length Transmembrane Domain. *Structure 21*, 1897−1904.